REFERENCES

1. R.W. Lyles and J.H. Wyman. Evaluation of Speed Monitoring Systems. FHWA, Final Rept. FHWA/PL/80/006, July 1980.
2. R.W. Lyles and J.H. Wyman. Evaluation of Vehicle Classification Equipment. FHWA, Final Rept., July 1982.
3. J.F. Scarzello and G.W. Usher, Jr. Self-Powered Vehicle Detector: Magnetic Sensor Development. FHWA, Rept. FHWA-RD-76-147, June 1976.
4. J.H. Wyman and R.W. Lyles. Evaluation of the Self-Powered Vehicle Detector. FHWA, June 1981.
5. M.K. Mills. Magnetic Gradient Vehicle Detector. IEEE Transactions on Vehicular Technology, Vol. VT-23, No. 3, Aug. 1974.
6. M. Singleton and J.E. Ward. A Comparative Study of Various Types of Vehicle Detectors. U.S. Department of Transportation, Rept. DT-TSC-OST-77-9, Sept. 1977.
7. T. Takagi. Optical Sensing and Size Discrimination of Moving Vehicles Using Photocell Array and Threshold Devices. IEEE Transactions on Instrumentation and Measurement, Vol. 25, No. 1, March 1976.
8. K. Jakus and D.S. Coe. Speed Measurement Through Analysis of the Doppler Effect in Vehicular Noise. IEEE Transactions on Vehicular Technology, Vol. VT-24, No. 3, Aug. 1975.
9. M.R. Parker, Jr. An Evaluation of the Following Too Closely System. Traffic Engineering, Vol. 46, No. 7, July 1976.
10. John Hamburg and Associates. Improved Methods for Vehicle Counting and Determining Vehicle Miles of Travel--A Review of the Current State-of-the-Art on Vehicle Classification Programs. NCHRP, draft report, Oct. 1979.
11. Highway Performance Monitoring System: Case Study Procedural Manual--Vehicle Classification. Program Management Division, FHWA, Jan. 1980.
12. R.C. Moore. Road Sensors for Traffic Data Collection. Sensors in Highway and Civil Engineering. Institute of Civil Engineers, London, England, Paper 7, 1981.
13. R.C. Moore, P. Davies, and P.R. Salter. An Automatic Method to Count and Classify Road Vehicles. Presented at International Conference of Road Traffic Signalling, Institute of Electrical Engineers, London, England, March-April 1982.
14. Automatic Method to Classify, Count, and Record the Axle Weight of Road Vehicles. U.K. Transport and Road Research Laboratory, Crowthorne, Berkshire, England, Leaflet 639, 1979.
15. Road Sensor for Vehicle Data Collection: The Axle Detector. U.K. Transport and Road Research Laboratory, Crowthorne, Berkshire, England, Leaflet 905, 1979.
16. Automatic Vehicle Count and Classification: Examples of Data Output. U.K. Transport and Road Research Laboratory, Crowthorne, Berkshire, England, Leaflet 884, 1979.

Publication of this paper sponsored by Committee on Traffic Flow Theory and Characteristics.

Analysis of TRANSYT Platoon-Dispersion Algorithm

NAGUI M. ROUPHAIL

The development of an analytical solution to the recursive platoon-dispersion formula used in TRANSYT models of traffic flow is presented. Flow rates in the predicted platoon measured at the kth interval of the jth simulated cycle are expressed in terms of demand and capacity rates at the source intersection in addition to signal-control and travel-time parameters. It was found that the TRANSYT recursive formula implicitly contains a cycle factor that results in an underestimation of the toal flow rate simulated. An estimate of that error has been formulated, which can be applied as a constraint on the required simulation time in TRANSYT. The analytical solution also provided insight into the determination of critical intersection spacings below which signal coordination becomes feasible.

The proliferation of digital computer model applications in the areas of traffic flow and control in the past decade has led to the successful development of several widely used traffic signal operations models, such as Network Simulation Model (NETSIM), Signal Operations Analysis Package (SOAP), Traffic Network Study Tool (TRANSYT), and Traffic Signal Optimization Program (SIGOP) (1-4).

TRANSYT, a program for traffic signal timing and coordination initially developed in the United Kingdom by Robertson (5), has been successfully applied at many intersections in Europe and the United States. The TRANSYT-7F version, for example, has recently been used in the National Signal Timing Optimization Project (6), which encompassed 11 cities and approximately 500 signalized intersections in the United States.

The fundamental principle of traffic representation in TRANSYT-type models is platoon-dispersion behavior. Simply stated, as a queue of vehicles leaves the stopline on the green indication, its shape is altered along the downstream link in a manner reflective of the desire of individual drivers to maintain comfortable time headways. Thus, although the flow rate at the stopline is equivalent to the saturation rate in the presence of a queue and to the demand rate thereafter (assuming undersaturated operation), the flow patterns measured at an observation point t seconds downstream of the stopline would be considerably different.

Mathematically, platoon-dispersion behavior is expressed by the following recursive relationship:

$$IN(k + t) = F \times OUT(k) + (1 - F) \times IN(k + t - 1) \quad (1)$$

where

- IN(k + t) = flow rate in kth time interval of predicted platoon at observation point;
- OUT(k) = flow rate in kth time interval of original platoon at stopline;
- t = β times average platoon travel time from stopline to observation point [β is an empirical travel-time factor expressed as ratio between travel time of leading vehicle in platoon

and average travel time of entire platoon; a value of 0.8 has been suggested for use in TRANSYT models (7)]; and

F = empirically derived platoon-smoothing factor.

F is a function of travel time and geometric conditions on the link. To date, however, it has been expressed in terms of travel time only, as shown below:

$$F = 1/(1+\alpha t) \quad (2)$$

where α is the platoon-dispersion factor. Estimates of 0.50 and 0.35 were found to give the best fit to observed traffic under moderate travel friction in the United Kingdom and the United States, respectively. However, a recent U.S. study, described in a paper in this Record by McCoy and others, reported a correlation between the value of α and arterial geometries under low-friction traffic flow conditions. Values of $\alpha = 0.21$ and $\alpha = 0.14$ were suggested in the modeling of two-lane two-way and four-lane divided arterials, compared with the 0.25 value recommended in TRANSYT under the same conditions.

Thus the predicted flow rate at any time step is expressed as a linear combination of the original platoon flow rate in the corresponding time step (with a lag of t) and the flow rate of the predicted platoon in the step immediately preceding it.

The platoon-dispersion model formulated in Equation 1 has been successfully validated with field data collected in London and Manchester, England (8).

The objectives of this study thus may be stated as follows:

1. Develop a close-form solution to the platoon-dispersion algorithm in TRANSYT-type models,
2. Investigate the time-dependency impacts of the algorithm on the predicted platoon flow rates, and
3. Explore potential uses of the analytical expressions developed in the study for signal-coordination schemes.

The first step of the analysis was concerned with the determination of the platoon flow rates at the stopline of a signalized, isolated intersection, as discussed below.

FLOW RATES AT ISOLATED INTERSECTIONS

Consider the flow patterns occurring at an isolated signalized intersection (or peripheral intersection in a TRANSYT network), assuming undersaturated operation.

The following variables are defined:

c = cycle length (s),
g = effective green time (s),
r = effective red time (s),
λ = g/c,
g_s = saturated green time (s),
g_u = unsaturated green time (s),
n = number of time steps in a cycle as defined in TRANSYT,
q = average demand rate (vehicles/s),
s = saturation flow rate (vehicles/s),
y = q/s,
x = degree of saturation (= y/λ),
IN(k,j) = arrival rate in step k of cycle j, and
OUT(k,j) = departure rate in step k of cycle j.

Based on the flow profiles indicated in Figure 1, it can be shown that

$$sg_s = q(r + g_s) \text{ or } g_s = rq/(s - q) = ry/(1 - y)$$

Since $r = c - g = c(1 - \lambda)$,

$$g_s = cy(1 - \lambda)/(1 - y) \quad (3)$$

It is assumed that the red interval is made up of k_1 time steps. Therefore,

$$k_1 x(c/n) = r = c(1 - \lambda)$$

or

$$k_1 = n(1 - \lambda) \quad (4)$$

Similarly, k_2 is defined as the last time step in the saturated portion of the green phase, measured from the beginning of the effective-red interval. Thus

$$k_2 \, x \, (c/n) = r + g_s$$

or with some manipulation,

$$k_2 = n(1 - \lambda)/(1 - y) \quad (5)$$

Finally, let k_3 be the last time step in the cycle. By definition,

$$k_3 = n \quad (6)$$

Thus the following flow rates are used to describe the original platoon flow in step k of cycle j at the "source" intersection:

$$IN(k, j) = q \quad 1 \leq k \leq n, \text{ for all } j \quad (7)$$

$$OUT(k, j) = o \quad 1 \leq k \leq n(1 - \lambda), \text{ for all } j \quad (8)$$

$$OUT(k, j) = s \quad n(1 - \lambda) < k \leq n(1 - \lambda)/(1 - y), \text{ for all } j \quad (9)$$

$$OUT(k, j) = q \quad n(1 - \lambda)/(1 - y) < k \leq n, \text{ for all } j \quad (10)$$

Note that under fully saturated conditions (i.e., $\lambda = y$), the outflow rate described in Equation 10 is eliminated.

ANALYTICAL SOLUTION DEVELOPMENT

Case for Initial Cycle

The inflow rate in step k of the first simulated cycle measured at an observation point t seconds

Figure 1. Flow patterns at isolated intersection.

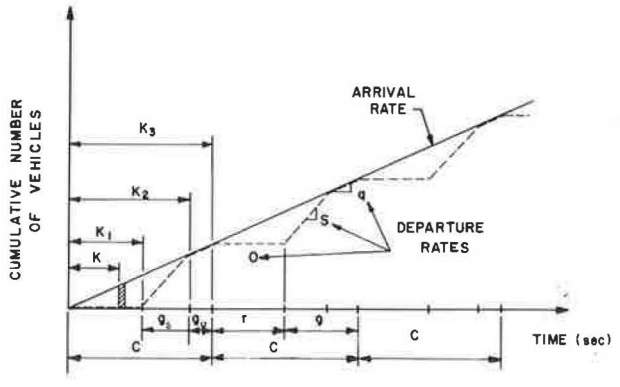

downstream of the stopline is expressed mathematically by Equation 1, rewritten below:

$$IN(k + t, 1) = F \times OUT(k, 1) + (1 - F) \times IN(k + t - 1, 1) \quad (1a)$$

From Equation 8, it is evident that no departures occur in the red interval; i.e.,

$$IN(k + t, 1) = 0 \qquad 1 \leq k \leq n(1 - \lambda) \quad (11)$$

The flow rate corresponding to the saturated portion of the effective-green phase is derived from Equation 9 as

$$IN(k + t, 1) = F \times s + (1 - F) \times IN(k + t - 1, 1)$$

Let k now be measured from the beginning of the effective-green phase and define the variable u_0 as

$$u_0 = IN[n(1 - \lambda) + t, 1]$$

where the subscript zero refers to the last step of the effective-red interval.

Substituting into Equation 1 gives

$$u_{0+1} = F \times s + (1 - F)u_0$$

$$u_{1+1} = F \times s + (1 - F)u_1$$

and, in general,

$$u_k = F \times s + (1 - F)u_{k-1}$$

Therefore,

$$u_k = (1 - F)^k u_0 + \sum_{\ell=0}^{k-1} F s(1 - F)^{\ell}$$

$$= (1 - F)^k u_0 + s[1 - (1 - F)^k]$$

When k is measured from the start of the red interval,

$$u_k = (1 - F)^{k-n(1-\lambda)} u_0 + s[1 - (1 - F)^{k-n(1-\lambda)}]$$

But from Equation 11, $u_0 = 0$; therefore,

$$IN(k + t, 1) = s[1 - (1 - F)^{k-n(1-\lambda)}] \qquad n(1 - \lambda) < k \leq n(1 - \lambda)/(1 - y) \quad (12)$$

The flow rate corresponding to the unsaturated portion of the green phase is derived from Equation 10 as

$$IN(k + t, 1) = F \times q + (1 - F) \times IN(k + t - 1, 1)$$

Let k be measured from the beginning of the unsaturated portion of the green phase and define $\acute{u}_0$ as

$$\acute{u}_0 = IN\{[n(1 - \lambda)/(1 - y)] + t, 1\}$$

where the subscript zero refers to the last step of the saturated green time.

From Equation 12, it can be shown that

$$\acute{u}_0 = s\{1 - (1 - F)[n(1 - \lambda)/(1 - y)] - n(1 - \lambda)\}$$

$$= s\{1 - (1 - F)[ny(1 - \lambda)/(1 - y)]\} \quad (13)$$

Proceeding in a similar fashion as that above for $\acute{u}_1$, $\acute{u}_2$, and so on gives

$$\acute{u}_k = (1 - F)^k \acute{u}_0 + \sum_{\ell=0}^{k-1} Fq(1 - F)^{\ell}$$

$$= (1 - F)^k \acute{u}_0 + q[1 - (1 - F)^k]$$

Substituting $\acute{u}_0$ from Equation 13 and letting k be measured from the start of the red interval,

$$IN(k + t, 1) = s[1 - (1 - F)^{ny(1-\lambda)/(1-y)}](1 - F)^{k-[n(1-\lambda)/(1-y)]} + q\{1 - (1 - F)^{k-[n(1-\lambda)/(1-y)]}\}[n(1 - \lambda)/(1 - y)] < k \leq n \quad (14)$$

A summary of the flow rates derived in this section is presented in Table 1. Note that the flow rates are valid only in the first simulated cycle in TRANSYT, as the subsequent analysis explains.

Case for Subsequent Cycles

If we refer to Table 1, it can be proved that

$$\sum_{k=1}^{n} IN(k + t, 1) < \sum_{k=1}^{n} OUT(k, 1) \text{ for } 0 \leq t \leq \infty$$

This is primarily due to the recursive nature of the platoon-dispersion formula itself, which continuously incorporates a fraction of all previous flow rates in the calculation of the predicted platoon. Thus the difference

$$\sum_{k=1}^{n} OUT(k, 1) - \sum_{k=1}^{n} IN(k + t, 1)$$

may be viewed as a residual flow from cycle 1 that will be dispersed in cycles 2, 3, ..., j according to the dispersion formula in Equation 1. The same reasoning may be applied for platoons generated in the second and subsequent cycles throughout a simulation run.

Thus for a particular cycle j, the flow rate in the predicted platoon at time (k + t) may be viewed as the sum of two components:

1. Flow rate due to the original platoon generated in step k of cycle j at the source intersection and
2. Residual flow rate from all previous platoons generated in cycle 1, 2, ..., j - 1 at the source intersection.

The first component is identical to the flow rate generated in the first simulated cycle, i.e., with no consideration of previous platoons. This concept is illustrated graphically in Figure 2, which depicts the progression of a platoon downstream of an isolated intersection and the associated residual flows generated in each cycle.

The residual flow rate from the ith cycle that occurs in step k of the jth cycle (j > i), $R_{i,j,k}$, can be expressed by the following equation:

$$R_{i,j,k} = IN(n + t, 1) \times (1 - F)^{k+n(j-i-1)} \quad (15)$$

For example, letting i = 1, j = 2 gives

$$R_{1,2,k} = IN(n + t, 1) \times (1 - F)^k$$

Table 1. Platoon-flow boundary values.

Case	Travel Time	$k_1 \leq k \leq k_2$	Q_∞[a]
1	0	$1 \leq k \leq n(1 - \lambda)$	Zero
2	0	$n(1 - \lambda) < k \leq [n(1 - \lambda)/(1 - y)]$	$qc(1 - \lambda)/(1 - y)$
3	0	$[n(1 - \lambda)/(1 - y)] < k \leq n$	$qc(\lambda - y)/(1 - y)$
4	∞	Same as 1	$qc(1 - \lambda)$
5	∞	Same as 2	$qcy(1 - \lambda)/(1 - y)$
6	∞	Same as 3	$qc(\lambda - y)/(1 - y)$

[a] $Q_\infty = (c/n) \sum_{k=k_1}^{k_2} IN(k + t, \infty)$.

Figure 2. Platoon-dispersion formula characteristics.

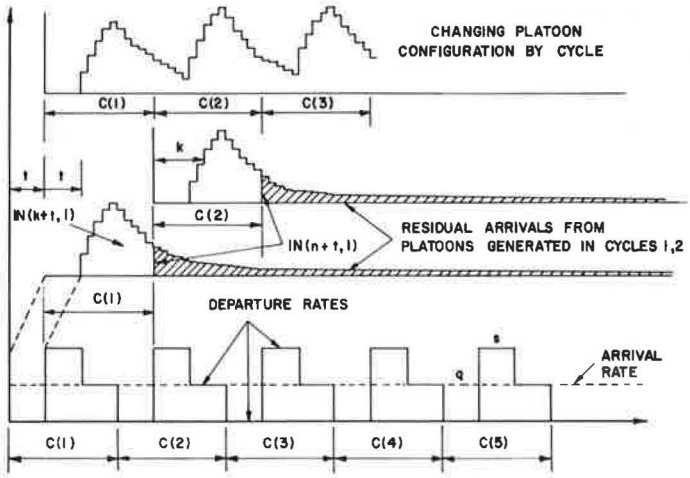

Figure 3. Summary of flow rates for initial cycle.

Region[a]	Boundaries for (k)	OUT(k,1)	IN(k+t,1)
1	$1 \le k \le n(1-\lambda)$	0	0
2	$n(1-\lambda) < k \le \frac{n(1-\lambda)}{(1-y)}$	s	$s\left[1 - (1-F)^{k-[n(1-\lambda)]}\right]$
3	$\frac{n(1-\lambda)}{(1-y)} < k \le n$	q	$s\left[1 - (1-F)^{ny(1-\lambda)/(1-y)}\right] \times (1-F)^{k-[n(1-\lambda)/(1-y)]} + q\left[1 - (1-F)^{k-[n(1-\lambda)/(1-y)]}\right]$

[a] 1 = Red phase at source intersection
2 = Saturated portion of green phase
3 = Unsaturated portion of green phase

which is consistent with Equation 1 since the OUT(k,1) term is eliminated when cycle 2 is considered.

Therefore, the total flow rate in the predicted platoon, including residuals from all previous cycles, is expressed as

$$IN(k+t,j) = \left(\sum_{i=1}^{j-1} R_{i,j,k}\right) + IN(k+t,1) \quad (16)$$

which suggests that the flow rates (and consequently the actual number of vehicles) simulated in TRANSYT appear to be systematically related to the length of a simulation run.

Solving Equation 16 for j = 2,3,4, respectively, gives

$$IN(k+t,2) = IN(n+t,1)(1-F)^k + IN(k+t,1)$$

$$IN(k+t,3) = \left(\sum_{i=1}^{2} R_{i,3,k}\right) + IN(k+t,1) \quad (17)$$

But from Equation 15,

$$R_{1,3,k} = IN(n+t,1) \times (1-F)^{k+n}$$

$$R_{2,3,k} = IN(n+t,1) \times (1-F)^k$$

Therefore, it can be shown that

$$IN(k+t,3) = IN(n+t,1)(1-F)^k\,[1 + (1-F)^n] + IN(k+t,1) \quad (18)$$

A similar derivation for j = 4 gives

$$IN(k+t,4) = IN(n+t,1)(1-F)^k\,[1 + (1-F)^n + (1-F)^{2n}] + IN(k+t,1) \quad (19)$$

which leads to a general expression for cycle j, j > 1:

$$IN(k+t,j) = \left[IN(n+t,1)(1-F)^k \sum_{m=0}^{j-2} (1-F)^{mn}\right] + IN(k+t,1)$$

$$= IN(n+t,1)(1-F)^k \left\{[1-(1-F)^{n(j-1)}]/[1-(1-F)^n]\right\} + IN(k+t,1) \quad (20)$$

Equation 20 is a general platoon-dispersion formula that predicts the flow rate in the kth step ($1 \le k \le n$) of the jth simulated cycle in TRANSYT. Because the term containing the cycle designation j vanishes at j = 1, the expression is considered valid for any cycle, including the initial one.

By substituting the values of IN(n + t,1), IN(k + t,1) from Figure 3, the set of general expressions for flow rates is realized. A summary of these is presented in Figure 4.

CYCLE FACTOR AND ERROR ESTIMATION

The dependency of platoon flow rate on cycle designation implies that each time an IN histogram is

Figure 4. General expressions for flow rates.

Cycle (j)	Region[a]	$k_1 \leq k \leq k_2$	OUT(k,j)	IN(k+t,j)
1	1*	$1 \leq k \leq n(1-\lambda)$	0	0
	2*	$n(1-\lambda) < k \leq \frac{n(1-\lambda)}{(1-y)}$	s	$s\left[1-(1-F)^{k-n(1-\lambda)}\right]$
	3*	$\frac{n(1-\lambda)}{(1-y)} < k \leq n$	q	$s\left[1-(1-F)^{ny(1-\lambda)/(1-y)}\right](1-F)^{k-[n(1-\lambda)/(1-y)]} + q\left[1-(1-F)^{k-[n(1-\lambda)/(1-y)]}\right]$
> 1	1	$1 \leq k \leq n(1-\lambda)$	0	$(1-F)^k\left[\frac{1-(1-F)^{n(j-1)}}{1-(1-F)^n}\right]\left\{q\left[1-(1-F)^{n(\lambda-y)/(1-y)}\right] + s(1-F)^{n(\lambda-y)(1-y)} \times \left[1-(1-F)^{ny(1-\lambda)/(1-y)}\right]\right\}$
	2	$n(1-\lambda) < k \leq \frac{n(1-\lambda)}{(1-y)}$	s	$s\left[1-(1-F)^{k-n(1-\lambda)}\right] + (1-F)^k\left[\frac{1-(1-F)^{n(j-1)}}{1-(1-F)^n}\right] \times \left\{q\left[1-(1-F)^{n(\lambda-y)/(1-y)}\right] + s(1-F)^{n(\lambda-y)/(1-y)} \times \left[1-(1-F)^{ny(1-\lambda)/(1-y)}\right]\right\}$
	3	$\frac{n(1-\lambda)}{(1-y)} < k \leq n$	q	$s\left[1-(1-F)^{ny(1-\lambda)/(1-y)}\right](1-F)^{k-[n(1-\lambda)/(1-y)]} + q\left[1-(1-F)^{k-[n(1-\lambda)/(1-y)]}\right] + (1-F)^k\left[\frac{1-(1-F)^{n(j-1)}}{1-(1-F)^n}\right] \times \left\{q\left[1-(1-F)^{n(\lambda-y)/(1-y)}\right] + s(1-F)^{n(\lambda-y)/(1-y)} \times \left[1-(1-F)^{ny(1-\lambda)/(1-y)}\right]\right\}$

[a] 1 = Red signal indication at source intersection. 2 = Queue released on green indication (g_s in eq. 3). 3 = Vehicles Released at arrival rate on green indication.

constructed in TRANSYT from essentially the same OUT patterns, the resulting flow rates will be different. This time dependency is reflected in Equation 20 by the term $[1-(1-F)^{n(j-1)}]$, hereafter designated the cycle factor.

To demonstrate the impact of the cycle factor on the number of vehicles generated in a TRANSYT run, consider a simulation period lasting m cycles. Since the total number of vehicles leaving the stopline each cycle is qc, the total number of vehicles simulated is mqc. At an observation point t seconds downstream of the stopline, the corresponding number of vehicles arriving in cycle j can be calculated as follows:

$$Q_j = (c/n) \sum_{k=1}^{n} IN(k+t, j) \tag{21}$$

and the total number of vehicles simulated in m cycles is

$$Q = \sum_{\ell=1}^{m} Q_\ell \tag{22}$$

The relative cycle error based on m simulated cycles (E_m) is now defined as

$$E_m = [qc - (Q/m)]/qc \times 100 \text{ percent} \tag{23}$$

where Q/m is the average number of vehicles generated per cycle in the predicted platoon, based on a simulation run lasting m cycles.

The variable Q_j in Equation 21 has been calculated for the three flow patterns considered at the source intersection. The results are tabulated in Figure 5.

In order to ascertain the validity of the total flow expressions of Q, two special cases were considered:

1. Travel time is zero (F = 1): In this case, the IN flow value in Equation 21 should duplicate the OUT flow values at the source intersection.
2. Travel time is infinity (F = 0): In this case, the IN flow values in Equation 21 should duplicate the IN flow values that occur at an isolated intersection.

In both cases, cycle dependency was considered negligible, since j was set to infinity. Formulas for the two cases are summarized in Table 1.

Proof: Based on the OUT patterns derived in Equations 8 through 10, the total flow generated at the source intersection can be expressed as follows:

$$Q_1 = \sum_{k=1}^{n(1-\lambda)} 0 \times (c/n) \qquad 1 \leq k \leq n(1-\lambda) \tag{24}$$

$$Q_2 = \sum_{k=[n(1-\lambda)]+1}^{n(1-\lambda)/(1-y)} s \times (c/n) \qquad n(1-\lambda) < k \leq [n(1-\lambda)/(1-y)] \tag{25}$$

$$Q_3 = \sum_{[n(1-\lambda)/(1-y)]+1}^{n} q \times (c/n) \qquad [n(1-\lambda)/(1-y)] < k \leq n \tag{26}$$

It can be readily shown that the values of Q_1, Q_2, and Q_3 correspond precisely to expressions 1, 2, and 3 given in Table 1.

Proceeding in a similar fashion for $t = \infty$, it is observed that the q multipliers in expressions 4, 5, and 6 are actually the durations of the red, saturated-green, and the unsaturated-green intervals, respectively, at the source (and in fact isolated) intersection. In other words, the flow rate in each of the three regions has a fixed value q throughout the cycle, a distinct feature of the isolated-intersection arrival-flow pattern.

A computer program was written to calculate the relative cycle error (E_m) for a variety of travel-

Figure 5. Number of vehicles generated in predicted platoons.

Region	$k_1 \le k \le k_2$	$Q_j = \frac{c}{n} \sum_{k_1}^{k_2} IN(k+t,j)$
1	$1 \le k \le n(1-\lambda)$	$\frac{c}{n}\left\{\frac{1-(1-F)^{n(j-1)}}{1-(1-F)^{n}} \times \frac{(1-F)}{F} \times \left[1-(1-F)^{n(1-\lambda)}\right] \times \left(q\left[1-(1-F)^{n(\lambda-y)/(1-y)}\right] + s(1-F)^{n(\lambda-y)/(1-y)} \times \left[1-(1-F)^{ny(1-\lambda)/(1-y)}\right]\right)\right\}$
2	$n(1-\lambda) < k \le \frac{n(1-\lambda)}{(1-y)}$	$\frac{c}{n}\left\{\frac{qn(1-\lambda)}{(1-y)} + \left\{\left(\frac{1-(1-F)^{n(j-1)}}{1-(1-F)^{n}} \times q\left[1-(1-F)^{n(\lambda-y)/(1-y)}\right] + s(1-F)^{n(\lambda-y)/(1-y)} \times \left[1-(1-F)^{ny(1-\lambda)/(1-y)}\right]\right) - \frac{s}{(1-F)^{n(1-\lambda)}}\right\} \times \left(\frac{(1-F)^{n(1-\lambda)+1}}{F} \times \left[1-(1-F)^{ny(1-\lambda)/(1-y)}\right]\right)\right\}$
3	$\frac{n(1-\lambda)}{(1-y)} < k \le n$	$\frac{c}{n}\left\{\frac{qn(\lambda-y)}{(1-y)} + \left\{s\left[1-(1-F)^{ny(1-\lambda)/(1-y)}\right] + \left\{\frac{\left[1-(1-F)^{n(j-1)}\right]}{1-(1-F)^{n}} \times \left(q\left[1-(1-F)^{n(\lambda-y)/(1-y)}\right] + s(1-F)^{n(\lambda-y)/(1-y)} \times \left[1-(1-F)^{ny(1-\lambda)/(1-y)}\right]\right)\right\}\right\} \times \left(\frac{(1-F)^{n(1-\lambda)+1}}{F} \times \left[1-(1-F)^{n(\lambda-y)/(1-y)}\right]\right)\right\}$

Figure 6. Relative cycle error for t = 20 s.

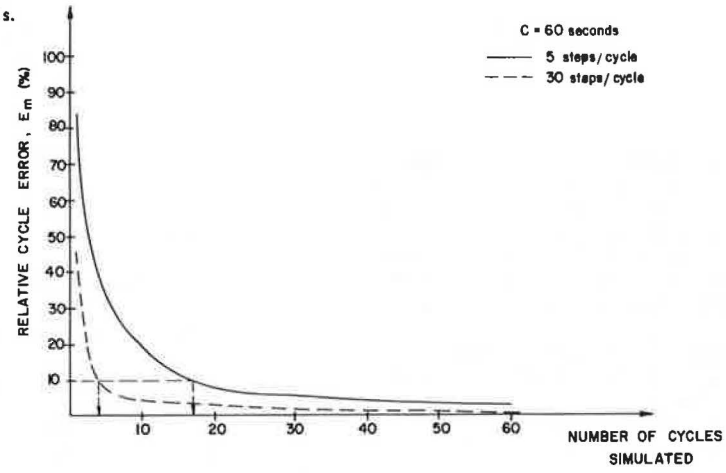

time, signal-control, and simulation-run parameters. The results are depicted graphically in Figures 6 and 7. These graphs are useful in the preliminary determination of the required duration of a simulation run, so as to maintain the relative cycle error below a prespecified threshold. For example, for a pair of intersections that are 20 s apart (under free-flow conditions), a relative cycle error of 10 percent will not be exceeded if a simulation period is selected that is (a) 4 cycles long, each made up of 30 steps, or (b) 17 cycles long, each made up of 5 steps. The corresponding values for a travel time of 60 s are 11 steps and 49 cycles.

It was also noted that the cycle error is virtually independent of the degree of saturation at the source intersection, at least within the degree of saturation range tested in this study ($0.55 \le x \le 1.00$). Thus in a simulation of a TRANSYT network, the controlling factor in the selection of required simulation time and interval duration is in fact the highest link travel time. Once an acceptable cycle error is attained for that critical link, all other links in the network will automatically satisfy that same requirement.

Of course, if the analytical expressions derived in this study were to substitute for the recursive relationship in TRANSYT, under steady-state cycle conditions (i.e., $j = \infty$), then the cycle error would be totally eliminated.

SIGNAL COORDINATION FEASIBILITY LIMITS

The derivation of analytical solutions to the platoon recursive formula makes it possible to study

Figure 7. Relative cycle error for t = 60 s.

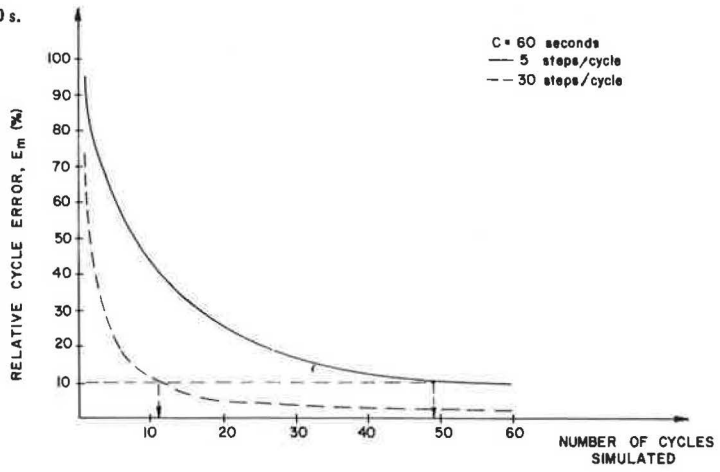

Figure 8. P_I versus travel-time functions for x = 0.625.

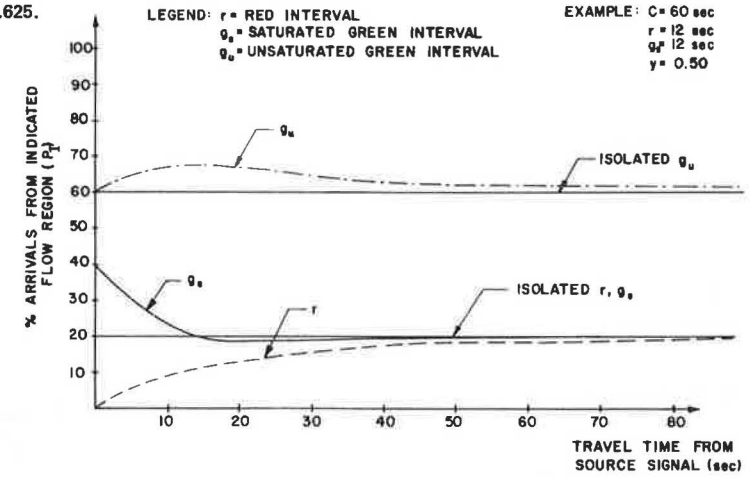

the potential value of providing signal coordination between the source intersection and a hypothetical destination intersection located within t seconds of travel. This is accomplished by comparing the actual flow rates arriving at the destination intersection with the predicted flow rates had the destination intersection been considered isolated in nature.

Consider a time interval of length r that corresponds to the red signal indication at the source intersection. For an isolated intersection, the proportion of vehicles arriving in r (P_r) is simply the proportional duration of interval r to the cycle length (c). In other words,

$$P_r = c(1 - \lambda)/c = 1 - \lambda \quad (27)$$

Now if we consider the actual proportion of arrivals in interval r based on platoon dispersion after time t ($P_{r,t}$), it can be shown that

$$P_{r,t} = Q_{\infty,r} / \sum_{i=1}^{3} Q_{\infty,i} \times 100 \text{ percent} \quad (28)$$

where $Q_{\infty,i}$ is the steady-state ($j = \infty$) number of vehicle arrivals at the destination intersection that originated in interval i (i = 1,2,3) at the source intersection. Q-values are depicted in Figure 5.

Similar expressions are developed for vehicle arrivals corresponding to the saturated (g_s) and unsaturated (g_u) portions of the green interval, as follows:

$$P_{g_s} = cy(1 - \lambda)/c(1 - y) = y(1 - \lambda)/(1 - y) \quad (29)$$

$$P_{g_s,t} = (Q_{\infty,g_s} / \sum_{i=1}^{3} Q_{\infty,i}) \times 100 \text{ percent} \quad (30)$$

$$P_{g_u} = c(\lambda - y)/c(1 - y) = (\lambda - y)/(1 - y) \quad (31)$$

$$P_{g_u,t} = (Q_{\infty,g_u} / \sum_{i=1}^{3} Q_{\infty,i}) \times 100 \text{ percent} \quad (32)$$

The values of P_I, where I denotes a general interval, are plotted against free-flow travel time between source and destination intersections in Figures 8 and 9 by using three different demand/capacity ratios.

The graphs clearly demonstrate that the source platoon rapidly degenerates (with time) into a uniform flow pattern, although theoretically the two patterns coincide only at t = ∞. It is also observed that the rate of platoon degeneration is dependent on the degree of saturation at the source intersection; in general, a platoon degenerates more rapidly at higher degrees of saturation.

To the extent that the platoon-dispersion formula in TRANSYT is valid, Figures 8 and 9 may be used to investigate intersection spacing thresholds for signal coordination. There is no attempt in this paper to develop any such guidelines, in part because of the narrow scope of the numerical examples depicted in the figures. However, as additional data are successfully tested, a mathematical model with

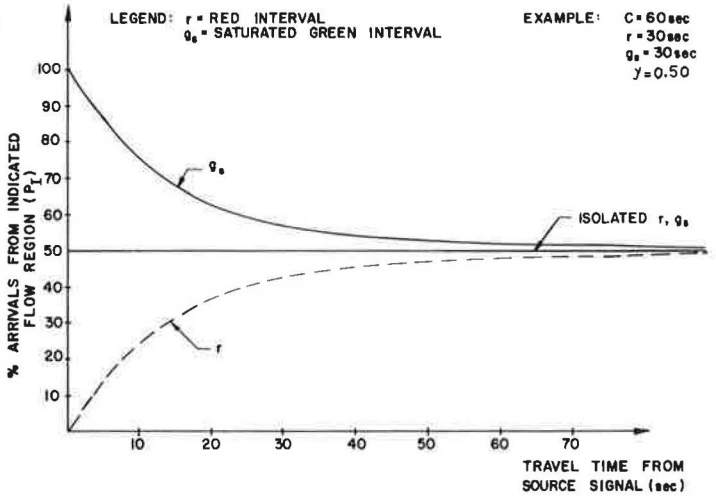

Figure 9. P_I versus travel-time functions for x = 1.00.

Table 2. Cycle dependency of queue lengths and delays: numerical example.

Variable	Cycle			
	1st	3rd	10th	50th
Average flow rate in predicted platoon[a] (vehicles/s)	0.032	0.210	0.247	0.249
Average flow rate in green interval[b] (vehicles/s)	0.064	0.221	0.253	0.255
Average queue length[c] (vehicles)	0	2.58	3.55	3.63
Uniform vehicle delay [vehicles/(s·cycle)]	0	154.8	213.0	217.8

[a] Average at source intersection = 0.25 vehicle/s.
[b] Assuming zero green offset between intersections and green interval of 30 s.
[c] Queue length is zero in first cycle since all arrivals occur in the green interval at the destination intersection.

travel time and degree of saturation as independent variables and a measure of the absolute difference between P_I and $P_{I,t}$ as the dependent variable could be used directly to estimate the value of providing signal coordination between a pair of intersections.

ILLUSTRATIVE EXAMPLE

The following numerical example demonstrates the impact of cycle error on the magnitude of uniform vehicle delay, which is a component of the performance index in TRANSYT. Mathematically, delay is expressed as follows:

$$d_u = (c/n) \sum_{k=1}^{n} m_k \quad (33)$$

where d_u is the uniform delay in vehicles per second per cycle and m_k is the queue length during step k in vehicles c, n, k as defined earlier. m_k is calculated as follows:

$$m_k = \max \{m_k - 1 + (c/n)\,[IN(k) - OUT(k)], 0\} \quad (34)$$

Thus, for a pair of intersections operating under a simultaneous-progression pattern (i.e., offset = 0) and identical g/c ratios, it is assumed that c = 60 s, g = 30 s, t = 60 s, n = 10, α = 0.35, q = 900 vehicles/h (0.25 vehicle/s), and s = 1800 vehicles/h (0.50 vehicle/s).

By using the flow equations shown in Figure 4, the predicted platoon-arrival rates at the destination intersection were calculated. When these IN flow rates were overlaid on the OUT patterns (that is, zero offset, g/c = 0.50 at the destination intersection), queue length and delay estimates were obtained by using Equations 33 and 34.

This procedure was carried out for platoons generated in the 1st, 10th, and 50th cycles of a simulated TRANSYT run. The results are summarized in Table 2.

The average flow rates, queue lengths, and uniform delays exhibited virtually identical variations with cycle number. All were underestimated in cycles 1, 2, and 3. Between the 3rd and the 10th cycles, all performance measures were within 5 percent of their terminal values reached at the later cycles. The location of a knee (point of substantial slope change) in the delay-versus-cycle relationship may be viewed as a desirable upper limit on the simulation time beyond which little will be gained in terms of computational accuracy of the performance measures.

Further work is planned regarding an investigation of cycle-factor impact on the final TRANSYT settings, which was beyond the scope of this paper.

CONCLUSIONS

An analytical solution to the recursive platoon-dispersion formula used in TRANSYT-type models has been developed in this paper.

The findings of the study have potential significance in several aspects of macroscopic traffic simulation modeling:

1. The recursive relationship in TRANSYT contains a time-dependent factor, which in turn underestimates the total flow generated in a simulation run and consequently all performance measures (such as delays and stops) associated with it. The analytical expressions developed in the study give a precise measurement of that factor.
2. Time dependency of flow rates generated in TRANSYT may be reduced by increasing the simulation period, the number of steps per cycle, or both when the recursive relationship is used. As an option, however, it is possible to use the analytical expressions derived in this study under steady-state cycle conditions (i.e., assuming an infinite number of runs), which thus eliminates the time-dependency effect.
3. A number of expressions developed in this study describe the process by which a platoon of vehicles degenerates into a uniform-flow pattern. The rate of degeneration was found to increase with the degree of saturation at the source intersec-

tion. Mathematical models are suggested to evaluate signal coordination feasibility limits between a pair of intersections.

ACKNOWLEDGMENT

This study was supported in part by a University of Illinois at Chicago Research Board Grant.

REFERENCES

1. E. Lieberman and others. NETSIM Model--User's Guide. FHWA, Rept. FHWA-RD-770-44, 1977.
2. Signal Operations Analysis Package--User's Manual. FHWA, 1979.
3. D.I. Robertson. TRANSYT: A Traffic Network Study Tool. British Road Research Laboratory, Crowthorne, Berkshire, England, Rept. BRRL 25S, 1969.
4. Peat, Marwick, Livingstone and Co. SIGOP: Traffic Signal Optimization Program--User's Manual. U.S. Bureau of Public Roads, 1968. NTIS: PB 182835.
5. D.I. Robertson. Contribution to Discussion on Paper 11. Presented at Symposium on Area Control of Road Traffic, Institution of Civil Engineers, London, 1967.
6. National Signal Timing Optimization Project: Executive Summary. ITE Journal, Vol. 52, No. 10, Oct. 1982.
7. TRANSYT-7F User's Manual. FHWA, Feb. 1981.
8. P.A. Sneddon. The Prediction of Platoon Dispersion in the Combination Methods of Linking Traffic Signals. Transportation Research, Vol. 6, 1972, pp. 125-130.

Publication of this paper sponsored by Committee on Traffic Flow Theory and Characteristics.

Optimization Model for Isolated Signalized Traffic Intersections

W.B. CRONJÉ

The existing methods for the optimization of isolated fixed-time signalized traffic intersections are applicable either to undersaturated stationary conditions or to oversaturated conditions. As far as is known, no model exists that is applicable to all conditions. A model is developed for the optimization of fixed-time signalized intersections that is applicable to undersaturated as well as to oversaturated conditions. In the model, the macroscopic approach to traffic flow is used. Although it is not so accurate as the microscopic approach, values are obtained for delay and number of stops that are accurate enough for practical purposes and that use much less computer time. Macroscopic simulation is then approximated by the geometric probability distribution. In this case also, values for delay and number of stops are obtained that are accurate enough for practical purposes and that use much less computer time. Consequently, the geometric probability distribution model is recommended for the optimization of fixed-time signalized traffic intersections.

The purpose of this paper is the development of a model for the optimization of fixed-time signalized intersections.

Most of the research in the field of signalized intersections has been done for undersaturated conditions. In this paper, however, we shall not refer to specific shortcomings, but as a result of these shortcomings, it has been decided to develop an accurate model for practical application to undersaturated and oversaturated conditions.

First, microscopic and macroscopic simulation are compared in the stationary zone with reference to average delay and number of stops. The difference is found to be negligible for practical purposes, and macroscopic simulation is used in the further development of the model because it uses much less computer time.

Second, average delay and number of stops are determined by macroscopic simulation in the nonstationary zone. Good agreement is found between the values obtained at the end of the nonstationary zone and those in the stationary zone. Macroscopic simulation in the nonstationary zone can therefore be deemed correct (see Figure 1).

Last, macroscopic simulation is approximated by the geometric probability distribution to further reduce computer time. Good agreement is found for all practical purposes, and the geometric model is therefore recommended for the optimization of fixed-time signalized intersections.

COMPARISON BETWEEN MICROSCOPIC AND MACROSCOPIC SIMULATION

Macroscopic traffic flow at a signalized intersection is indicated in Figure 2, which shows average arrivals per unit time interval (q), overflow of vehicles at the end of the previous cycle (Q_B), overflow of vehicles at the end of the cycle (Q_E), cycle length (c) in seconds, effective green time (g) in seconds, effective red time (r) in seconds, and saturated flow (s) in vehicles per second. The total delay per cycle (D) is the area under the queue-length diagram:

$$D = [(2 \cdot Q_B + q \cdot r)r/2] + [(q \cdot r + Q_B + Q_E)g/2] \quad (1)$$

The number of stops per cycle (N) is the number of vehicles that arrive while there is a queue plus the overflow at the start of the cycle (Q_B):

$$N = c \cdot q + Q_B \quad (2)$$

Microscopic traffic flow is indicated in Figure 3.

In the macroscopic case, arrival of vehicles per cycle is obtained by generating random numbers. In the microscopic case, gaps between vehicles are obtained similarly.

By working from a zero origin, the times of arrival and departure are obtained; thus the delay is experienced. By summation of the delay for all vehicles, the total delay (D) is obtained. The average delay (d) is then the total delay divided by the sum of all the vehicles arriving during the period considered.

The number of stops is obtained as follows.